JURNAL SEGARA
http://ejournal-balitbang.kkp.go.id/index.php/segara

ISSN : 1907-0659
e-ISSN : 2461-1166
Acreditation Number : 158/E/KPT/2021

ACOUSTIC WAVE PROPAGATION PATTERNS IN THE OCEAN COLUMN

Fachri Ali Badihi[1)], Sri Pujiyati[1)], Ayi Rahmat[1)], Steven Solikin[1)], & Muhammad Hisyam[2)]

[1)]Department of Marine Science and Technology, IPB University, Dramaga, Bogor, 16680 West Java, Indonesia
[2)]Department of Marine and Fisheries Sciences, Cenderawasih University, Heram, Jayapura, 99224, Papua, Indonesia

Received: 8 August 2022; Revised: 20 December 2022; Accepted: 23 December 2022

ABSTRACT

Temperature and salinity play a role in the speed of sound and the process of sound propagation of acoustic waves in the water. Research on the propagation of sound waves in the ocean is a very interesting topic to do because it has many applications, including in underwater wireless communication systems and maritime security. This study aimed to analyze the propagation of acoustic waves in different water depths. The modeling was carried out with flat wave characteristics, in which the bathymetry characteristics of the seawater were ignored. In this ray path simulation, the frequency of 5.3Hz was used at 3 stations with different seawater depths in the Makassar Strait using temperature and salinity data downloaded from marine.copernicus.eu data. The movement pattern of the acoustic waves was simulated using the Bellhop method. The ray tracing simulation results showed significant differences at the three locations. This was influenced by several factors, including the condition of the seawater environment, the placement of the transducer, the speed of sound, and the depth. Shallow seawater would show a more complicated ray path than deep seawater. The greater the angle of the half beam used, the greater the distance of the range of each beam of light will be so that the reflection of the resulting beam of light covers each column of seawater. The closer the distance between the resulting ray paths, the smaller the energy lost.

Keywords: Acoustic Wave, Temperature, Salinity, Ocean Column, Raypath, Makassar Strait.

Corresponding author:
Jl. Pasir Putih I Ancol Timur, Jakarta Utara 14430. Email: sirpu@apps.ipb.ac.id

INTRODUCTION

Based of Indonesia's bathymetric profile and the characteristics of its seawater mass, Indonesia is an archipelagic country with various types of seawater. The Makassar Strait is geographically located between the islands of Borneo and the island of Sulawesi, connecting the Pacific Ocean through the Sulawesi Sea with the Java Sea and the Flores Sea (Inaku, 2015). The seawaters of the Makassar Strait are interesting for research because they are the location of the entry of the Indonesian Throughflow seawater mass (Horhoruw *et al*., 2015; Inaku, 2015). Based on its bathymetry, the Makassar Strait has different depth profiles, from shallow to depths of more than 2000 m.

Temperature and salinity are factors that can be observed in marine seawaters. The difference in seawater depth will affect the vertical temperature and salinity profile, as well as the density of the seawater mass in it. This condition will also affect the speed of sound and the acoustic wave propagation pattern in the seawater column. According to Lurton (2002), the pattern of vertical sound wave propagation is as follows: (a) in the mix layer, the speed of sound is high on the surface, then the mixed layer decreases and is relatively constant, (b) In the thermocline layer, the speed decreases drastically following changes in fluctuating temperature, usually the temperature decreases drastically in a relatively shallow depth range, (c) In the deep layer, the speed of sound waves increases with increasing depth due to pressure hydrostatic.

The Bellhop method is a method that can predict acoustic wave propagation based on a Gaussian beam, which is used to mathematically model an acoustic wave channel as an information carrier medium in an underwater wireless communication system. This Gaussian beam equation is useful for modeling a range-dependent condition, namely a condition where the parameters affect the propagation of the acoustic wave, namely the value changes with increasing distance from the source. This study aims to analyze the propagation of acoustic waves at different seawater depths.

METHODOLOGY

This study used marine.copernicus.eu data which was downloaded on January 1st, 2021. The data were taken from three station points in the Makassar Strait (Figure 1) with the coordinates showed in Table 1. The data in the form of temperature, salinity and current. This research was conducted from January 1 to February 28, 2021 at the Marine Acoustics, Instrumentation and Robotics Division, Department of Marine Science and Technology, Faculty of Fisheries and Marine Sciences, IPB University.

Table 1. Three Research Stations

Stations	Latitude	Longitude	Depth
1	0°43'39.8"N	119°24'195"E	2,225 m
2	1°36'58.5"S	117°55'33.3"E	1,684.3 m
3	3°37'02.2"S	117°29'49.5"E	1,452.3 m
Source: personal documentation			

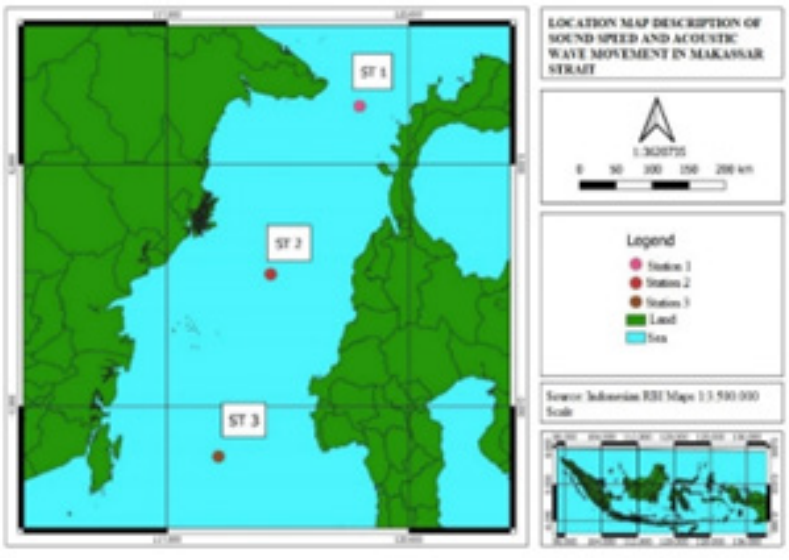

Figure 1. Stations for data collection in Makassar Strait waters. Source: Personal Documentation

The tools used for data processing were laptops with Intel Core i3 processor specifications with 6 GB RAM, simulation programs and other data processing programs. The materials used were time series temperature and salinity data for a month (1st-31st July 2020) and currents downloaded from the marine.coperniccus.eu web page in the Makassar Strait.

The sound wave propagation pattern is a parameter that is frequency independent, so that the shape of the sound wave propagation pattern for all frequencies is the same. The thing that distinguishes the shape of the sound wave propagation pattern is the profile of the speed of sound, depth, angle and characteristics of the bottom / sea surface. In this study, the modeling was carried out with flat wave characteristics, in which the bathymetric characteristics of the seawater were ignored. In the simulation of this sound wave propagation pattern, a frequency of 5.3Hz was used because Stations 1, 2 and 3 have high seawater depths. The number of beams was 65 with a basic density of 1.025 g/cm^3 and a basic attenuation of 0.8 db/λ then the parameters used in the simulation to see changes in the movement of acoustic waves. The depth of placement of the transducer was at 1000 m, with 3 different half-beam angles (5°,15° and 30°), and then we ran a simulation with the results in the form of a graph so that analysis could be carried out to draw conclusions.

Calculation of the speed of sound was using the equation by Mackenzie (1981).

$$C = 1448.96 + 5.304 \times 10^{-2}T^2 + 2.374 \times 10^{-4}T^3 + 1.34(S-35) + 1.630 \times 10^{-2}Z + 1.675 \times 10^{-7}Z^2 - 1.025 \times 10^{-2}T(S-35) - 7.139 \times 10^{-13}TZ^3 \quad ..\ 1)$$

Sound waves can be bent or refracted as they travel. This happens because the sound waves propagate through two media that have different densities, resulting in a deflection of the direction of propagation. In propagation through two different mediums, Snell's law applies as follows:

$$\frac{v_1}{\sin\theta_1} = \frac{v_2}{\sin\theta_2} \quad ....\ 2)$$

RESULTS AND DISCUSSION

The three points of data collection stations were in the northern, central, and southern parts of the Makassar Strait. The three stations had different depths (2215.1 m, 1684.3 m, and 1452.3 m). Based on Figure 2, the three stations have different current speeds and current directions. The magnitude and direction of the current are influenced by the width of the strait and the topography of the seawater. The surface current at Station 1 was a swift current that came from the north, where the main seawater mass source is from the North Pacific Ocean. Station 2 also had the same swift current speed as Station 1, where Station 2 has a deep depth and is far from the mainland, and also there are no barriers. At Station 3, the current tended to be weaker than at Stations 1 and 2. This was due to a barrier that changed the direction and speed of the current at that location. Yuliarinda *et al*., 2012 stated that both stations 1 and 2 are far from the mainland, have a deep depth, and there are no barriers, so the wind blows strongly, which causes the current to tend to be stronger. While June-july coincides with the East Season in the Makassar Strait, the average surface current pattern is more dominant to the south of the sea (Mahie, 2005).

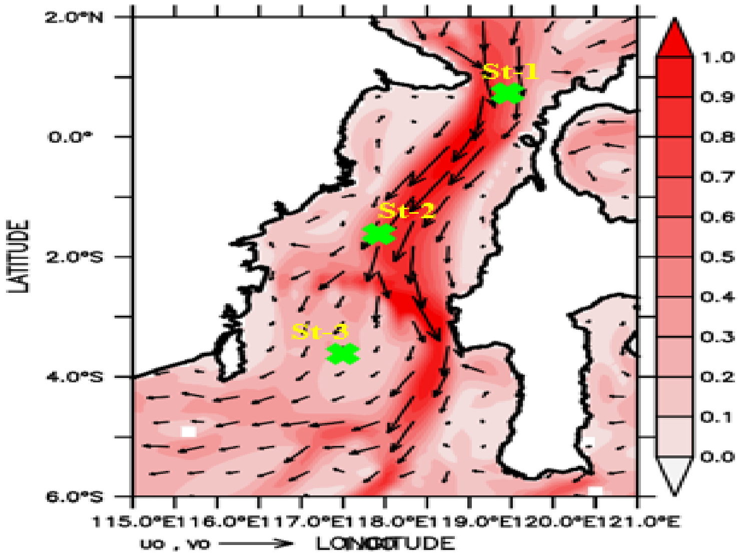

Figure 2. Surface Current in Makassar Strait in July 2020. Source: Measurement results

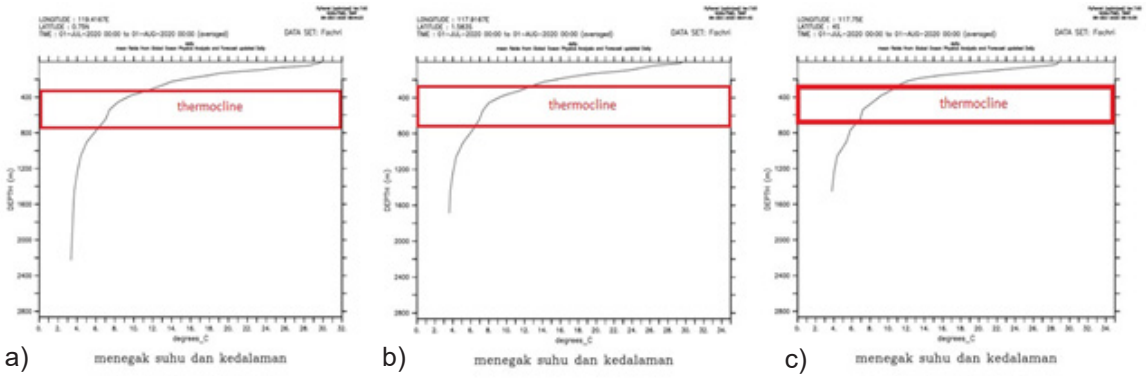

Figure 3. Temperature and depth profile in the Makassar Strait (a) Station 1; (b) Station 2; (c) Station 3.
Source: Measurement results

Figure 3 shows the temperature profile with respect to depth. In general, there were mixed layer, thermocline, and deep layer areas. As seen in the figure, the temperature tends to decrease with increasing depth. At depths of close to 100 m to 200 m, the temperature decreased quite sharply at a fairly narrow depth and was thought to be a thermocline layer. At more than 200 m, the temperature decreased relatively constant with increasing depth. The temperature in the Makassar Strait ranged from 27°C to 30°C that was according to research done by Gunawan *et al*. (2019) that ranged from 25° to 29°. June-July coincides with the East Season, which has a relatively lower temperature. This was due to the presence of a North Pacific water mass with a very dominant low temperature characteristic passing through the Makassar Strait (Akhlak *et al*., 2015; Putra *et al*., 2012). Inaku (2015) said that in the Makassar Strait, there is upwelling that occurs due to the Southeast Munson wind, which forces the seawater mass in the lower seawater column to rise to the surface.

Figure 4 shows the vertical profile of salinity against depth. The salinity value on the surface was in the range of 34-34.2 psu, which can be seen at the three stations. This range is also in accordance with the study by Gunawan *et al*. (2019) that majority in range around 34 psu. The highest salinity value was in the depth range of 100-200 m. It was suspected that this is the thermocline layer where the salinity value reaches 34.7 psu. In this layer, the salinity would fluctuate. When approaching a depth of 600 m, salinity would increase slowly with increasing depth. According to Pickard & Emery (1990), maximum salinity in tropical seawaters occurs at a depth of 100–200 m, close to the thermocline layer. During the East Season, North Pacific transport seawater with high salinity characteristics was very dominant through the Makassar Strait (Putra, Kunarso, & Rita, 2020). In addition, the southern region of the Makassar Strait tends to experience an upwelling process that occurs due to the Southeast Munson wind that forces the mass of seawater in the higher salinity seawater column rises to the surface.

Based on sound speed equation, the value of the speed of sound is obtained as shown in Figure 5. The speed of sound showed the similarity at each station. When the depth was less than 60 m, the speed of sound in the three stations tended to be constant, which is also called a mix layer. Mixing of seawater masses caused by stirring by the wind. At depths approaching a depth of 100–200 m, the speed of sound at three stations decreased sharply due to the thermocline area. Above a depth of 200 m, the speed of sound decreased to a depth of 900 m at all stations. According to Urick (1983), the lowest sound speed is located in the deep

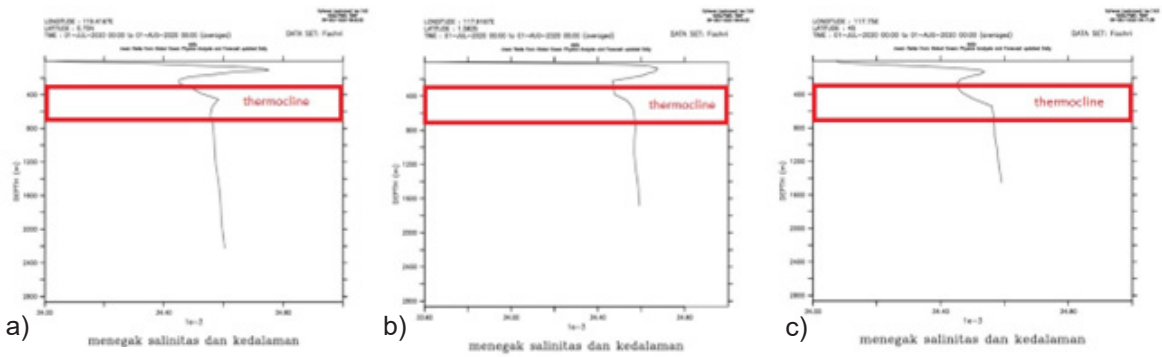

Figure 4. Salinity and depth profile in the Makassar Strait. (a) Station 1; (b) Station 2; (c) Station 3.
Source: Measurement results

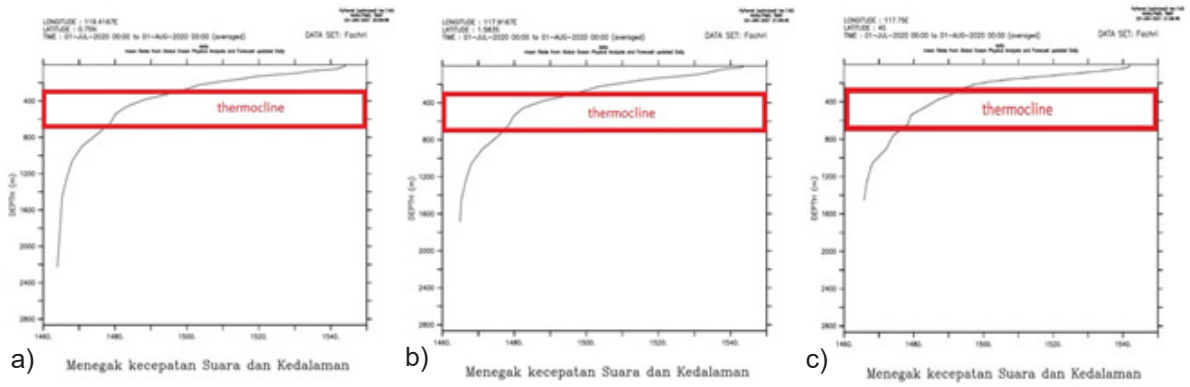

Figure 5. The profile of the speed of sound and depth in the Makassar Strait (a) Station 1; (b) Station 2; (c) Station 3. Source: Measurement results

voice canal at a depth that varies from 1,219.2 m at middle latitudes to near the surface in the polar region. At a depth of 900 m, the speed of sound will begin to be affected by depth (pressure), so that the speed of sound will increase as the depth increases. In addition, the decrease in temperature and the increase in salinity proceed very slowly. At station 1, the speed of sound was between 1544 m/s and 1464 m/s. Station 2 had a sound speed range of between 1543 m/s and 1465 m/s. Station 3 had a sound speed range of between 1542 m/s and 1466 m/s.

Medwin & Clarence (1998) stated that temperature, salinity, and depth affect the speed of sound in the seawater column. Waite (2005) said that the speed of sound in seawater is also influenced by location, season, time, and weather. These four factors affect the characteristics of the seawater that affect the speed of sound. The speed of sound in the East Season has a deep gradient of the speed of sound, temperature, and salinity that have a greater influence than the effect of depth on the thermocline layer. Stewart (2008) stated that pressure has more effect on the speed of sound than the depth of sound. As the depth of sound increases, the speed of sound will increase.

Several limitations were used in the simulation of sound wave propagation, namely: (a) the same horizontal range of 50,000 m, (b) seawater depth of more than 1000 m, (c) the position of the sound source and receiver at the same depth of 1000 m, (d) Take-off angle (half beam) of the source used at 5°, 15°, and 30°, and (e) the same number of beam beams, namely 65 beams. The selection of these environmental limits and parameters was based on seeing their effects on the sound propagation process so that we could compare the results of the simulation of sound wave propagation based on the difference in the half beam angle used.

Figure 6 shows the simulation of sound wave propagation at the three stations. Figure 6a, Figure 6d, and Figure 6g show the shape of the ray path generated by the 5° half beam angle. Figure 6b, Figure 6e, and Figure 6h show the shape of the ray path generated by the 15° half beam angle. Figure 6c, Figure 6f, and Figure 6i show the shape of the ray path generated by the 30° half beam angle. Figures 6a, 6b, 6d, 6e, 6g, and 6h show that the ray path is blue, so that the ray path only touches the bottom at the three stations. The ray path will propagate with a bottom bounce path type, which means the ray path will be reflected by the seabed to the receiver by propagating on the seabed only. This was because the gradient of the sound speed profile used was negative so that the ray path would propagate in a downward propagation direction.

Figures 6c, 6f, and 6i show that the ray path is blue, followed by black and black. The blue color indicates that the ray path only touches the bottom, while the black color indicates that the ray path touches the surface and the bottom (both boundaries) of the sea. The black color of the ray path was because the velocity of sound gradient was an iso velocity gradient, i.e., there was no change in the value of the speed of sound or the value of the velocity of sound was the same. The value of the sound velocity gradient depends on environmental parameters including temperature, salinity, and seawater depth (pressure), so that acoustic wave propagation can increase or decrease in speed depending on the above factors.

The nine images have differences, namely the image produced from a 5° half beam angle (Figures. 6a, 6d, and 6g) produces a ray path beam that passes through a higher density level than the image produced by a 15° half beam angle (Figures. 8b, 8e, and 8h) and a half beam angle of 30° (Figs. 6c, 6f, and 6i). The density level was influenced by the beam angle used. The smaller the angle of courtship of the ray path, with the same number of beams emitted, the closer it will be. This was because the adjacent distance will get closer, so that the density value will increase and vice

versa. The image produced from a half beam angle of 5° (Figures 6a, 6d, and 6g) had a regular reflected light beam and the invisible medium was exposed to the beam, or what is also called the shadowzone, while the image produced by the half beam angle of 15° (Figures 6b, 6e, and 6h) had more irregular reflections than Figure 6a, so they covered each medium and produced a smaller shadowzone, as well as a 30° half beam angle (Figures 6c, 6f, and 6i).

This is still related to the use of a beam angle that was getting bigger with the distance of each beam getting farther away, so that the reflection of the resulting beam of light covered each medium. The farther the distance and the deeper the depth, the more reflection and the less energy. According to Defrianto & Pratama (2019), a shadow zone is an area that cannot propagate or bend sound waves so that they can almost not propagate in a medium due to various factors, such as reflection, refraction, and absorption of sound waves by the seawater column. When sound waves propagate through different densities, the sound waves will be reflected or refracted, so that the speed of sound has an important role in the acoustic wave propagation pattern (Linda *et al*., 2019; Nurdiyanto *et al*., 2011; Yuwono *et al*., 2012).

Acoustic propagation at the three stations had different characteristics. This is caused by several factors, including sea depth, medium, speed of sound and beam angle (Harianto *et al*., 2020; Suharyo, 2018; Wijaya, 2010) Based on seawater depth, Station 1 has a sea depth of 2,225.1 m (Figure 6a), which is the deepest station of the two other stations, while Station 2 and 3 have shallower depths. Station 2 has a sea depth of about 1684.3 m (Figure 6d), which is deeper than Station 3 (Figure 6g). Station 3 has a depth of 1452.3 m, which is the shallowest of the three stations compared. Deep and shallow sea depths had different propagation channel characteristics. The deeper the sea conditions, the more free the sound signal will propagate. Figure 6a, 6d, and 6g produce ray paths that can propagate to

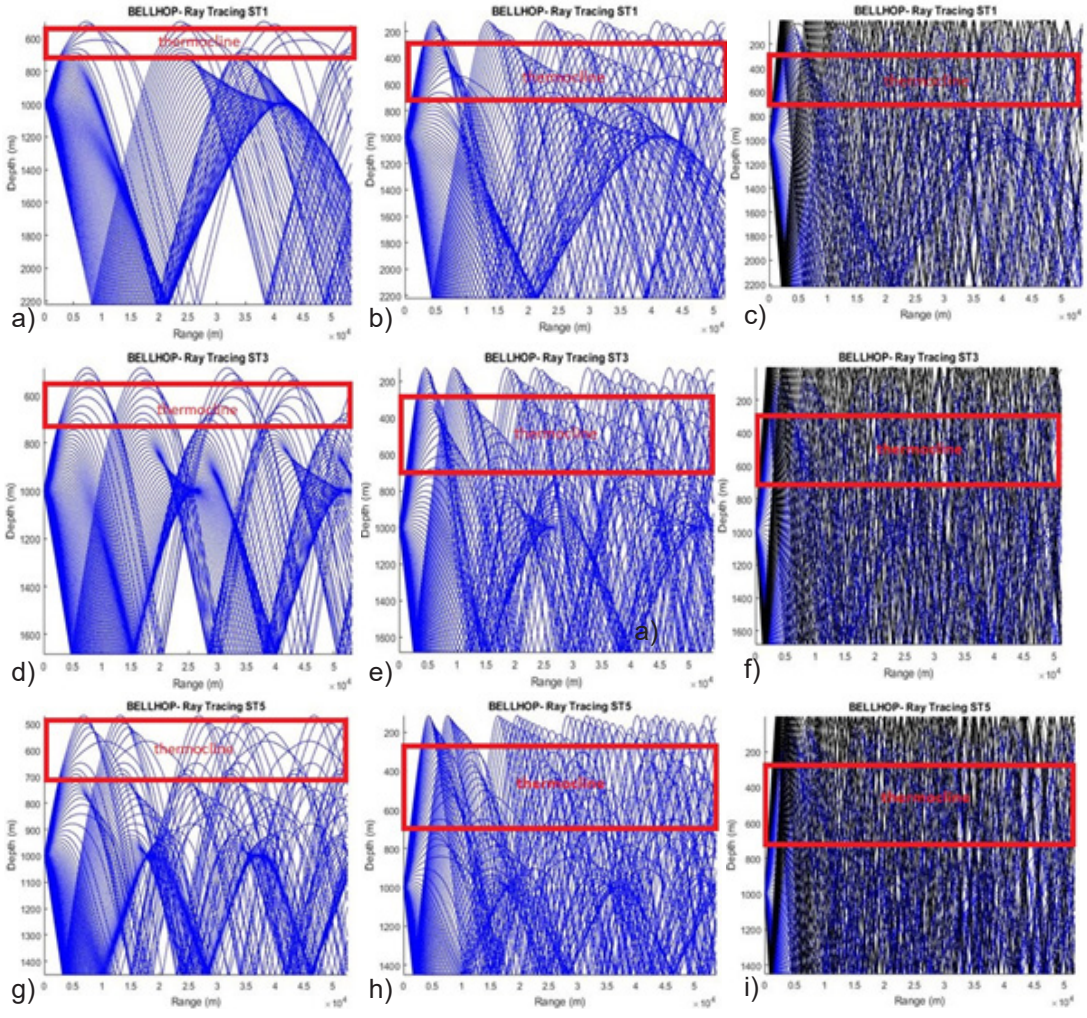

Figure 6. Sound Wave Propagation Pattern Simulation Results Station 1 with half beam angle (a) 5°; (b) 15°; (c) 30°. Station 2 with half beam angle (d) 5°; (e) 15°; (f) 30°. Station 3 with half beam angle (g) 5°; (h) 15°; (i) 30°. Source: Measurement results

the seabed and experience reflections.

Based on the speed of sound, in Figure 6a, 6d, and 6g, the ray clusters appear to form neat ray paths with close spacing between ray paths compared to Figure 6b, 6c, 6e, 6f, 6h, and 6i. The closer the distance between the resulting ray paths, the smaller the energy lost. The speed of sound at Station 1 is greater than at Stations 2 and 3, so that the energy lost will be smaller than at Station 2 and 3. This underwater acoustic propagation pattern depends on the speed of sound, so temperature has the same effect on the movement pattern of acoustic waves (Suharyo, 2018).

Based on the width of the beam angle, the wider or larger the angle used, the distance of each ray beam will move away and produce a more tenuous ray path. Figure 6a has a denser ray path than Figures 6b and 6c. Figure 6d has a denser ray path than Figures 6e and 6f. Figure 6g has a denser ray path than Figures 6h and 6i. The differences between the three stations can be seen at Station 1 (Figures 6a, 6b, and 6c), which had denser ray paths than Stations 2 (Figures 6d, 6e, and 6f) and Station 3 (Figures 6g, 6h, and 6i). Station 2 had a denser ray path than Station 3.

CONCLUSION

The pattern of acoustic wave movement simulation results using the Bellhop method compared with the results in the form of ray tracing shows a significant difference. This is influenced by several factors, including the medium, the placement of the transducer, the speed of sound, and the depth of the seawater. Based on the simulation results, shallow seawater will show a ray path that is more complicated than in deep seawater. The greater the angle of the half beam used, the greater the distance of the range of each beam of light would be, so that the reflection of the resulting beam of light covers each column of seawater. The closer the distance between the resulting ray paths, the smaller the energy lost.

ACKOWLEDGEMENTS

Thanks are expressed to all parties who have helped carry out the research and production of this article.

REFFERENCE

Akhlak, A.M., Supriharyono., & Hartoko, A. (2015). Relationship between variables of sea surface temperature, chlorophyll-a and catches of purse seine vessels that landed at the Bajomulyo Juwana TPI, Pati. *Diponegoro Journal of Maquares, 4*(4), 128-135.

Defrianto., & Pratama, N. (2019). Determination of the shadow zone area in the ocean computationally by simulating the propagation of acoustic rays. *Proceedings of SNFUR-4, 1*(1), 1-5.

Gunawan, I., Pranowo W. S., & Sukoco, N. B. (2019, in Indonesian). Study of Seawater Mass Characteristics in Eastern Indonesian Waters by Utilizing Argo Float Data. *Jurnal Chart Datum. 5*(2), 130-143. DOI: https://doi.org/10.37875/chartdatum.v5i2.151

Harianto, P.A., Eko, T.W., & Yumm, R.H. (2020). Effect of environmental conditions on the KRI's sonar ability to detect underwater contact. *Marine Journal, 3*(1), 1-10.

Horhoruw, S.M., Atmadipoera, A.S., Purba, M., & Purwandana, A. (2015). Current Structure and Spatial Variation of Indonesian Throughflow in Makassar Strait Under Ewin 2013. *Indonesian Journal of Marine Sciences, 20*(2), 87-100. https://doi .org/10.14710/ik.ijms.20.2.87-100

Inaku, D. F. (2015). Analysis of the distribution pattern and development of the upwelling area in the southern

Linda, F. N., Lepong, P., & Djayus. (2019). Interpretation of tomographic refractive seismic wave velocity in determining subsurface lithology in Bhuana Jaya Village (case study: PT. Khotai Makmur Insan Abadi). *Journal of Geosains, 2*(2).

Lurton, X. (2002). *An Introduction to Underwater Acoustics: Principles and Applications*. Praxis Publishing. Chichester.

Mackenzie, K.V. (1981). Nine-term equation for the sound speed in the oceans. *J. Acoust. Soc. Am. 70*(3), 807-812.

Mahie, G. A. (2005). Volume transport variation model (arlindo) in relation to the enso (el niño southern oscillation) in the Makassar Strait. *Journal of Mathematics, Statistics and Computing, 2*(1), 8-16.

Medwin, H., & Clay, C.S. (1998). *Fundamentals of Acoustical Oceanography*. Boston (US): Academia Permata.

Nurdiyanto, B., Hartanto, E., Ngadmanto, D., Sunardi, B., & Susilanto, P. (2011). Determination of rock hardness level using seismic refraction method. *Journal of Meteorology and Geophysics, 12*(3), 211-220.

Putra, E., Gaol, J. L., & Siregar, V. P. (2012). Relationship of chlorophyll-a concentration and sea surface temperature with the catch of major pelagic fish in Java Sea waters from MODIS satellite imagery. *Journal of Fisheries and Marine Technology, 3*(2), 1-10.

Putra, W. T., Kunarso, & Rita, T. D. (2020). Distribution of temperature, salinity and density in homogeneous and thermocline layers of Makassar Strait waters. *Indonesian Journal of Oceanography, 2*(2), 188-198.

Stewart, R.H. (2008). *Introduction to physical oceanography*. Department of Oceanography, Texas A&M University. 345p.

Suharyo, O.D. (2018). Effect of water mass movement and distribution. *Marine Journal, 11*(2), 104-112.

Urick, J. (1983). *Principle of Underwater Acoustic*. McGraw Hill, New York.

Yuliarinda, R.E, Muslim., & Atmodjo, W. (2012). Study of thermocline layer structure in Makassar Strait waters. *Journal of Oceanography, 1*(1), 34-39.

Yuwono, N. P., Arifianto, D., & Widjiati, E. (2012). Analysis of underwater sound propagation as a function of salt content and temperature. *Pomits Journal of Engineering, 1*(1), 1–3.

Waite, H.D. (2005). *Sonar for Practicing Engineers: Third Edition*. John Willey & Sons Ltd. West Sussex.

Wijaya, T.H. (2010, in Indonesian). *Analysis of the bellhop propagation model on underwater acoustic signal transmission*. thesis. Surabaya (ID): Institut Sepuluh Nopember Surabaya.